

Importance Sampling Analysis of PMD Outages in PDM-QPSK Coherent Nonlinear Transmissions

Stefan Wabnitz, *Member, IEEE*

Abstract—We numerically estimate, by the importance sampling technique, the polarization mode dispersion-induced outage probability in single-channel and hybrid wavelength division multiplexing 112-Gbit/s polarization division multiplexing-quadrature phase shift keying coherent nonlinear transmission systems without in-line dispersion management.

Index Terms—Nonlinear optics, optical fiber communication, polarization mode dispersion (PMD), quadrature phase shift keying (QPSK), wavelength division multiplexing.

I. INTRODUCTION

IN CURRENT 100 Gbit/s transmission systems employing polarization division multiplexing (PDM) and the quadrature phase shift keying (QPSK) modulation, compensation of the link chromatic-dispersion (CD) and polarization mode dispersion (PMD) is achieved by digital signal processing (DSP) at the coherent receiver. Other transmission impairments result from the fiber nonlinearity, i.e., self-phase modulation (SPM), cross-phase modulation (XPM) and cross-polarization modulation (XPoLM) among wavelength division multiplexing (WDM) channels.

Numerical simulations and experiments have shown that, in the case of dispersion-managed (DM) systems, nonlinear penalties in both single-channel and WDM (with 50 GHz channel spacing) 112 Gbit/s PDM-QPSK transmissions may be mitigated by introducing a moderate amount of fiber PMD [1]–[5]. However, since CD can be fully compensated at the receiver, it is convenient to eliminate in-line CD compensating fibers. Moreover, in non-DM systems, large dispersive signal spreading strongly reduces the impact of nonlinearities [1], [2], [5].

Yet, in spite of the use of DSP for the compensation of the average PMD, the statistical nature of PMD-induced bit-error-rate (BER) degradation requires the full knowledge of the associated probability density function (PDF). In particular, the knowledge of the tail of the BER-PDF is necessary in order to compute the PMD-induced outage probability (OP). The OP is associated with the presence of rare events, and its computation by means of conventional Monte Carlo simulation techniques is a prohibitive task. Hence the statistical

distribution of PMD-induced errors in 112 Gbit/s PDM-QPSK transmission systems with coherent receivers and DSP remains to date largely unexplored.

Recent studies have compared the performance of different electronic PMD equalizers by computing the residual OP by means of the multicanonical Monte Carlo (MMC) technique [6], [7]. The iterative nature of the MMC approach required intensive parallel computing, and was limited to studying the performance of a simple PMD emulator involving 30 birefringent waveplates.

We previously applied the importance-sampling (IS) technique [8] to the estimation of the PDF of the output Q factor in the presence of fiber nonlinearity, CD and PMD in nonreturn-to-zero (NRZ) on-off keying (OOK) systems [9]. In this letter, we extend the use of the IS technique to the case of PDM-QPSK coherent transmissions, which enables us to directly compute the PMD-induced OP in a realistic system setup involving CD, amplified spontaneous emission (ASE) noise, and fiber nonlinearity [5].

II. MODEL

Let us briefly present the model for a statistical study of the polarization interaction of WDM channels in the presence of fiber nonlinearity and PMD. Our simulations take into account all orders of PMD, four-wave mixing (FWM), SPM, XPM, XPoLM, CD, third order dispersion, and fiber attenuation. Fibers with random birefringence are divided into a series of different scattering sections of length, say, Δz_{scatt} with uniform birefringence. Wave propagation within each section is described by the two coupled nonlinear Schrödinger equations [10], [11]

$$\begin{aligned} & \left[\frac{\partial}{\partial z} + \frac{\alpha_{x,y}}{2} + \beta_{1x,y} \frac{\partial}{\partial t} - i \frac{\beta_2}{2} \frac{\partial^2}{\partial t^2} - \frac{\beta_3}{6} \frac{\partial^3}{\partial t^3} \right] E_{x,y}(t, z) \\ & = -i\gamma \frac{8}{9} \left[|E_{x,y}(z, t)|^2 + |E_{y,x}(z, t)|^2 \right] E_{x,y}(t, z) \end{aligned} \quad (1)$$

where $\alpha_{x,y}$ are the linear attenuations along the two fiber axes, $\beta_{1x,y}$ are the respective group velocities, $\beta_{2,3}$ are the CD and third order dispersion. Moreover, $\gamma = 2\pi n_2 / (\lambda A_{\text{eff}})$ is the fiber nonlinear coefficient, where n_2 is the nonlinear refractive index, λ is the wavelength and A_{eff} is the fiber effective area. The lengths of the scattering sections Δz_{scatt} are chosen from a random Gaussian distribution with a given mean value $\mu = 1$ km and the standard deviation $\sigma = 100$ m. The group velocities of the two polarization modes are related to the fiber PMD coefficient D_p as [11]

$$\beta_{1x} = -\beta_{1y} = \frac{D_p}{2\sqrt{\Delta z_{\text{scatt}}}}. \quad (2)$$

Manuscript received August 29, 2012; revised November 26, 2012; accepted December 11, 2012. Date of publication December 20, 2012; date of current version January 18, 2013. This work was supported in part by the Italian Ministry of University of Research under Grant 2008MPSSNX, in part by the Conseil Régional de Bourgogne, and in part by the iXCore Foundation.

The author is with the Department of Information Engineering, University of Brescia, Brescia 25123, Italy (e-mail: stefano.wabnitz@ing.unibs.it).

Color versions of one or more of the figures in this letter are available online at <http://ieeexplore.ieee.org>.

Digital Object Identifier 10.1109/LPT.2012.2234097

Linear propagation in each scattering section in presence of fiber birefringence is defined in terms of a frequency-dependent Jones matrix, whose eigenvectors specify the rotation axis in Stokes space. The angle θ between the rotation axis (or direction of the PMD vector) of a subsequent section with respect to the direction of the PMD vector at the output of the previous section is chosen as $\cos \theta = 2x^{1/\alpha} - 1$ where x is a random variable with uniform distribution in $[0, 1]$ and α is a bias parameter. Note that if $\alpha = 1$, then $\cos \theta$ has uniform distribution between $[-1, 1]$ (unbiased case). Whenever $\alpha > 1$, one obtains an angle distribution which is biased towards large differential group-delay (DGD) values [8], where the $DGD = D_p \sqrt{Z}$ and Z is the link length.

In order to be able to estimate with good accuracy the PMD-induced OP, it is necessary to postulate or calculate by numerical Monte-Carlo computation the PDF of the output BER in the presence of PMD. In practice it is not possible with simple Monte-Carlo simulations to accurately numerically evaluate the PDF of the BER, since in order to evaluate its tails one would need a prohibitively large number of simulations. On the other hand, the tails of the PDF can be computed with just a few thousands of simulations by the IS technique [8], [9].

III. SIMULATIONS

We simulated the propagation of a 112 Gbit/s PDM-QPSK channel at 193.1 THz over a 2000 km long standard-single mode fiber (SSMF) link without in-line CD compensation. The link comprised $N = 20$ identical, 100 km long spans of SSMF with dispersion coefficient $D = 16$ ps/nm/km, nonlinear index $\gamma = 1.3$ W⁻¹km⁻¹ and linear attenuation coefficient $\alpha = 0.2$ dB/km. The span loss was compensated by EDFAs with 7 dB noise figure. Cross-talk between the two polarization channels (resulting from possible misalignment between the polarization states of the channels and the polarization beam splitter in the polarization diversity receiver) was minimized by inserting an ideal state of polarization (SOP) controller after the link. This module restores the signal SOP affected by PMD, by applying to the input signal a polarization rotation matrix evaluated from the time-resolved comparison of the input signal SOP with the reference signal SOP at the given channel frequency.

In the simulations, the linewidth of transmitter and local oscillator lasers was equal to 1 MHz. On the other hand, we did not include a frequency offset between transmitter and local oscillator. We used an optical coherent quadrature receiver model, including the local oscillator, switchable polarization control, optical hybrids, postdetection electrical filters, DSP and Symbol Error Rate estimation. After coherent detection, DSP was performed on the electrical signal tributaries (I_x , Q_x , I_y , Q_y) by using: (i) fixed finite-impulse-response (FIR) filters for CD mitigation [12] with 2 samples per symbol after resampling, and $N = 800$ taps of the filter, which is consistent with the formula $N = 0.032B^2$ per 1000 ps/nm of CD at the Baud rate of B GBaud [13]; (ii) constant-modulus algorithm (CMA)-optimized multiple-input multiple-output (MIMO) equalizer for PMD and polarization cross-talk correction according to Eqs. (11–15) of ref. [13] with 2 samples per symbol after the analog-to-digital converter (ADC),

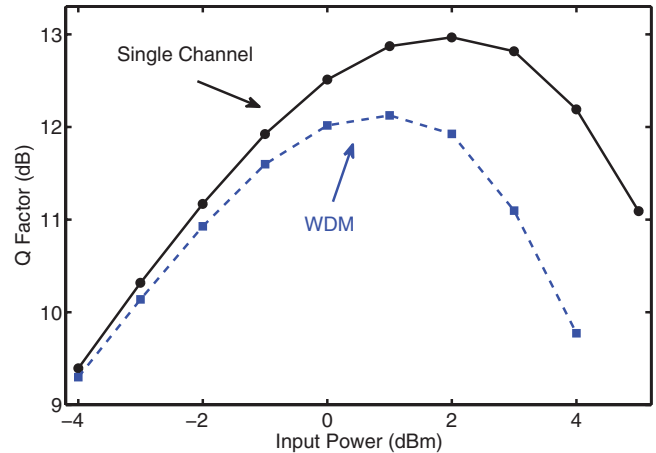


Fig. 1. Average output Q factor (in dB) of the 112 Gbit/s PDM-QPSK test channel versus input average channel power P_{in} , for single channel (black dots) and WDM (blue squares) transmissions. Lines are given as a guide.

$M = 11$ adaptive filter equalizer taps, a CMA convergence parameter $\mu = 5 \times 10^{-3}$, and a number of iterations $I_T = 30$; (iii) a Viterbi and Viterbi MSPE algorithm for phase noise estimation with $R = 2k + 1$ symbols used for phase estimation, where $k = 4$ is the number of pre-symbols [14], [15].

We simulated both single-channel and hybrid WDM transmissions (with 50 GHz channel spacing), where the central PDM-QPSK modulated signal at $B = 28$ GBaud (112 Gbit/s), generated using a pair of single drive Mach-Zehnder modulators, propagates along with two adjacent 14 Gbit/s NRZ-OOK channels, with their initial linear SOP oriented at 45° from the two PDM channels of the test 112 Gbit/s channel. The average power P_{in} of the NRZ-OOK side channels was kept equal to that of the central 112 Gbit/s channel. The PDM-QPSK signal comprised a random sequence of 1024 symbols, with 16 samples per symbol. Nonlinear propagation in the fiber in between any two subsequent polarization scattering sections was simulated with the Fourier split step method with a variable step size, so that the maximum phase change in the nonlinear step was kept below 0.05 rads. We represented the performance of the 112 Gbit/s PDM-QPSK test channel in terms of the quality factor $Q = 20 \log_{10} Q_{lin}$, where $Q_{lin} = \sqrt{2} \operatorname{erfc}^{-1}(2\text{BER})$ and the BER was estimated from the Monte Carlo simulations using the Gaussian assumption.

Fig. 1 shows the variation of the ASE noise-averaged output Q factor as a function of the average channel power for either single channel (black dots connected by a solid curve) or hybrid WDM transmission with two NRZ-OOK side-channels (blue squares connected by a dotted curve), respectively. In the simulations of Fig. 1 the PMD of the transmission fiber was set to zero. Fig. 1 shows that the optimal transmission performance is obtained for $P_{in} = +2$ dBm or $P_{in} = +1$ dBm in the single channel or the WDM case, respectively. Moreover, the XPolM from the presence of the two side channels leads to a peak performance degradation of about 1 dBQ. Note that the test channel average Q factor penalty due to XPolM by the side-channels is mostly due to its two immediate neighbors. Indeed, the Q factor curve of Fig. 1 with two WDM neighbors is almost identical to the corresponding curve of ref. [5], where the propagation of 8 side-channels was considered.

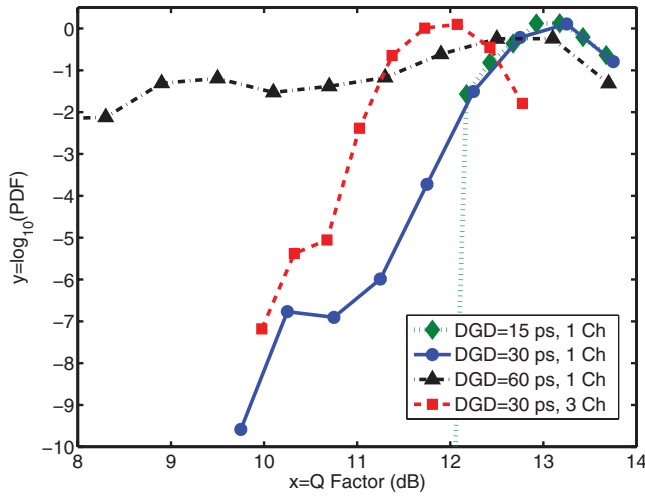


Fig. 2. Estimated PDF of the output Q factor of central 112 Gbit/s PDM-QPSK channel without or with two NRZ-OOK side channels, for different average DGD values. In all cases the channel average power $P_{in} = 2$ dBm.

In the presence of PMD, we studied by means of IS simulations the statistics of the output Q factor for the 112 Gbit/s PM-QPSK test channel at different values of the average DGD over the 2000 km link (see Fig. 2). The likelihood ratio L of each individual simulation was calculated as the product of the likelihood ratios of each fiber in the 20-span link

$$L = \prod_{i=1}^{20} L_i \quad (3)$$

where for each fiber

$$L_i = \prod_j (2/(\cos\theta_{ij} + 1))^{\alpha-1} / \alpha \quad (4)$$

and the index j denotes the scattering section. The PDF of the output Q factor was obtained by combining (using a simplified balance heuristic method [9]) the results of different PDFs obtained with either no bias ($\alpha = 1$), or with a given bias level (e.g., $\alpha = 1/(1-C)$ with $C = 0.1, 0.2$). For each set of unbiased or biased simulations we collected 1000 runs. As it can be seen in Fig. 2, PDF values as low as 10^{-10} can be easily reached by the IS technique for the PDF of the output Q factor. Moreover, it can be noticed that a good fit of the tail of the Q factor PDF is provided by a simple exponential law (i.e., a straight line in Figs. 2 and 3). By using this analytical fit for the tail of the PDF and its associated cumulative distribution, one may directly calculate the associated OP.

The IS simulations in Fig. 2 show that in the single channel case the average (over the action of noise and PMD) performance is degraded by 1 dB whenever the DGD increases from 30 ps up to 60 ps. Correspondingly, the tail of the Q factor PDF quickly grows larger when the DGD exceeds 30 ps. In fact, the OP (that we define as the probability that the performance is below the forward error correction (FEC) limit, i.e., the BER $> 2 \times 10^{-3}$ and $Q < 9.18$ dB) is as low as OP = 1.6×10^{-12} with the DGD = 30 ps and $P_{in} = +2$ dBm (see Fig. 3). From the exponential fit (not shown here) of the tail of the PDF in Fig. 2, we obtain that when the DGD = 60 ps, the OP = 4.4×10^{-2} . Such high OP value

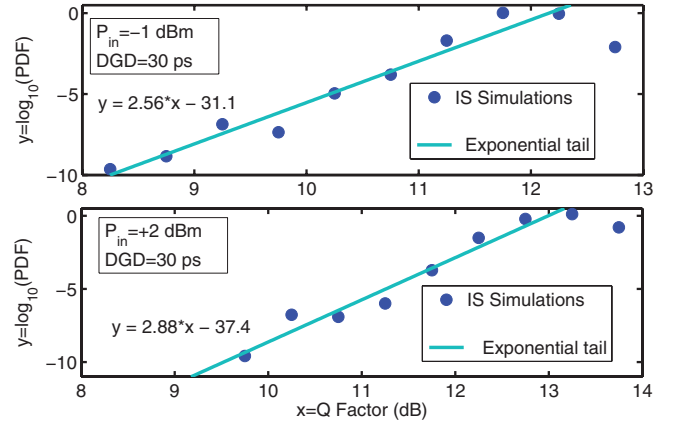


Fig. 3. Blue circles indicate the estimated PDF of the output Q factor for single channel 112 Gbit/s PDM-QPSK transmissions, with DGD = 30 ps, and $P_{in} = -1$ or $+2$ dBm.

could be reduced by increasing the complexity of the CMA-MIMO equalizer, i.e., the number of filter taps M [7], [8].

On the other hand, Fig. 2 shows that the decay rate of the Q factor PDF with DGD = 30 ps is slightly increased whenever two NRZ-OOK side channels are added to the central channel. Whereas the peak of the PDF is reduced by about 1 dBQ in the hybrid WDM case.

In order to see if nonlinearity affects the decay rate of the tail of the Q factor PDF, we compared in Fig. 3 the results of IS simulations for single channel 112 Gbit/s PDM-QPSK transmissions, where the channel power P_{in} is varied by 3 dB. Fig. 3 confirms that the tails of the PDF are relatively well approximated by an exponential decay in both cases. Moreover, the decay rate of these tails is virtually unaffected by decreasing P_{in} from $+2$ dBm down to -1 dBm; correspondingly, the outage probability is increased to OP = 4.3×10^{-9} . Therefore in non-DM QPSK systems the main effect of nonlinearity is the shift of the mean value of the PMD-induced PDF of the output Q factor. This is in contrast with the case of OOK systems in the presence of in-line DM and without PMD compensation, where it was shown that nonlinearity may strongly affect the width of the Q factor PDF as well [9].

Let us briefly discuss the dependence of the Q factor PDF in the presence of nonlinear cross-talk or XPolM from the two adjacent channels. Fig. 4 shows that when the two NRZ-OOK side channels are added, the average value of the PDF is nearly unaffected when increasing the DGD from zero up to 30 ps. On the other hand, in the WDM case the slope of decay of the exponential tail of the Q factor PDF is increased with respect to the single channel case in Figs. 2 and 3. As a result, in spite of the 1.2 dBQ decrease in the average Q value with respect to the single-channel case for $P_{in} = +2$ dBm which is shown in Fig. 1, in the WDM case the IS simulations predict that the outage probability is as low as OP = 1×10^{-12} , which is of the same order as the single channel OP. Thus, in analogy with the case of DM systems [1], [3]–[5], PMD may suppress nonlinear degradations to the OP in non-DM systems as well. This is due to the PMD-induced relative depolarization among the WDM channels which effectively washes out the effects of XPolM.

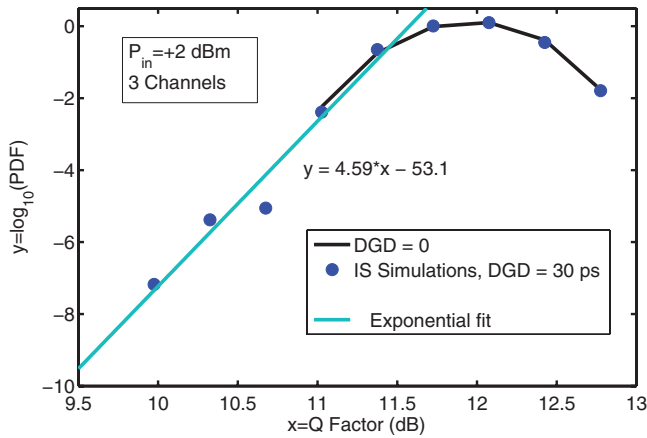


Fig. 4. Blue circles indicate the PDF of the output Q factor for the 112 Gbit/s PDM-QPSK channel with two NRZ-OOK 14 Gbit/s side channels and DGD = 30 ps. Black solid curve is obtained for DGD = 0.

IV. CONCLUSION

By means of the IS technique, we could numerically estimate the distribution of errors and the associated outage probability in both single-channel and hybrid WDM 112 PDM-QPSK transmissions with coherent receivers in systems without in-line dispersion management, in the presence of fiber nonlinearity and PMD. We found that in the WDM case, although the average performance is degraded by 1 dBQ by nonlinear XPolM, in the presence of PMD the outage probability may remain virtually unchanged with respect to the single-channel case.

Numerical simulations used the VPI Transmission Maker 8.7 software.

REFERENCES

- [1] P. Serena, N. Rossi, and A. Bononi, "Nonlinear penalty reduction induced by PMD in 112 Gbit/s WDM PDM-QPSK coherent systems," in *Proc. ECOC*, Vienna, Austria, 2009, pp. 1–2.
- [2] C. Xia, J. P. da S. Pina, A. Striegler, and D. van den Borne, "PMD-induced nonlinear penalty reduction in coherent polarization-multiplexed QPSK transmission," in *Proc. ECOC*, Torino, Italy, 2012, pp. 1–3.
- [3] O. Bertran-Pardo, *et al.*, "Demonstration of the benefits brought by PMD in polarization multiplexed systems," in *Proc. ECOC*, Torino, Italy, 2012, pp. 1–3.
- [4] O. Bertran-Pardo, *et al.*, "Linear and nonlinear impairment mitigation for enhanced transmission performance," in *Proc. OFC/NFOEC*, Los Angeles, CA, 2011, pp. 1–3.
- [5] P. Serena, N. Rossi, O. Bertran-Pardo, J. Renaudier, A. Vannucci, and A. Bononi, "Intra-versus inter-channel PMD in linearly compensated coherent PDM-PSK nonlinear transmissions," *J. Lightw. Technol.*, vol. 29, no. 11, pp. 1691–1700, Jun. 1, 2011.
- [6] N. C. Mantzoukis, C. S. Petrou, A. Vgenis, T. Kamalakis, I. Roudas, and L. Raptis, "Outage probability due to PMD in coherent PMD QPSK systems with electronic equalization," *IEEE Photon. Technol. Lett.*, vol. 22, no. 16, pp. 1247–1249, Aug. 15, 2010.
- [7] N. C. Mantzoukis, C. S. Petrou, A. Vgenis, I. Roudas, and T. Kamalakis, "Performance comparison of electronic PMD equalizers for coherent PDM QPSK systems," *J. Lightw. Technol.*, vol. 29, no. 11, pp. 1721–1728, Jun. 1, 2011.
- [8] G. Biondini, W. L. Kath, and C. R. Menyuk, "Importance sampling for polarization-mode dispersion: Techniques and applications," *J. Lightw. Technol.*, vol. 22, no. 4, pp. 1201–1215, Apr. 2004.
- [9] S. Wabnitz and K. S. Turitsyn, "Mitigation of nonlinear and PMD impairments by bit-synchronous polarization scrambling," *J. Lightw. Technol.*, vol. 30, no. 15, pp. 2494–2501, Aug. 1, 2012.
- [10] D. Wang and C. R. Menyuk, "Polarization evolution due to the Kerr nonlinearity and chromatic dispersion," *J. Lightw. Technol.*, vol. 17, no. 12, pp. 2520–2529, Dec. 1999.
- [11] D. Marcuse, C. R. Menyuk, and P. K. A. Wai, "Application of the Manakov-PMD equation for studies of signal propagation in optical fibers with randomly varying birefringence," *J. Lightw. Technol.*, vol. 15, no. 9, pp. 1735–1746, Sep. 1997.
- [12] S. Tsukamoto, K. Katoh, and K. Kikuchi, "Unrepeated transmission of 20-Gb/s optical quadrature phase-shift-keying signal over 200-km standard single-mode fiber based on digital processing of homodyne-detected signal for group-velocity dispersion compensation," *IEEE Photon. Technol. Lett.*, vol. 18, no. 9, pp. 1016–1018, May 1, 2006.
- [13] S. J. Savory, "Digital filters for coherent optical receiver," *Opt. Express*, vol. 16, no. 2, pp. 804–817, Jan. 2008.
- [14] A. J. Viterbi and A. M. Viterbi, "Nonlinear estimation of PSK-modulated carrier phase with application to burst digital transmission," *IEEE Trans. Inf. Theory*, vol. 29, no. 4, pp. 543–551, Jul. 1983.
- [15] S. Tsukamoto, K. Katoh, and K. Kikuchi, "Coherent demodulation of optical multilevel phase-shift-keying signals using homodyne detection and digital signal processing," *IEEE Photon. Technol. Lett.*, vol. 18, no. 10, pp. 1131–1133, May 15, 2006.